

## Synthesis, Assembly, and Thin Film Transistors of Dihydrodiazapentacene: An Isostructural Motif for Pentacene

Qian Miao,<sup>†</sup> Thuc-Quyen Nguyen,<sup>†</sup> Takao Someya,<sup>§</sup> Graciela B. Blanchet,<sup>‡</sup> and Colin Nuckolls<sup>\*†</sup>

Contribution from Department of Chemistry, Columbia University, New York, New York 10027, and DuPont, Central Research and Development, Wilmington, Delaware 19880

Received June 2, 2003; E-mail: cn37@columbia.edu

**Abstract:** The study below details the synthesis, assembly, and thin film transistors from dihydrodiazapentacenes. These molecules have the same molecular shape as pentacene but are much easier to prepare and have much greater environmental stability. Thin films made from the dihydrodiazapentacene behave as field effect transistors with mobilities and on/off ratios high enough to be useful in certain applications. X-ray diffraction and AFM experiments on these films show that the molecules stack in layers with their long axis upright from the surface. Some of the derivatives synthesized for this study have unexpectedly high solubility in polar solvents such as DMF and DMSO. The crystal structure from DMF reveals self-assembled channels with each of the aniline functionalities forming a hydrogen bond with solvent. In more nonpolar solvents, the solid-state assembly switches to a herringbone motif characteristic of the linear acenes.

### Introduction

The study below details the syntheses of a number of derivatives of dihydrodiazapentacenes (**2** and **3**) and their electrical response in thin films. Although some derivatives of these compounds have been known for over a century,<sup>1</sup> this study appears to be the first time that their electrical properties in thin films has been reported. The important finding is that some derivatives of these materials behave as organic field-effect transistors (FETs)<sup>2</sup> with on/off ratios greater than  $>10^4$  and mobilities approaching  $10^{-2} \text{ cm}^2\text{V}^{-1}\text{s}^{-1}$ . Thin-film organic FETs are useful because they can be deposited through a variety of techniques on flexible substrates over large area.<sup>3</sup> Some organic molecules have a sufficiently good electrical profile that they can be used as the drivers for individual pixels making them prime for applications such as electronic paper and large area displays.<sup>4</sup> Although certain compounds such as pentacene (**1**) and derivatives of oligothiophenes have been heavily

studied,<sup>2</sup> it is not clear if these molecules will ultimately be useful in devices because of a number of interrelated factors including low thermal stability, difficult derivatization, and facile atmospheric degradation.<sup>2,5,6</sup> Although high field effect mobility<sup>5</sup> is one important criterion for organic FETs, ultimate success in these organic transistors will require a holistic approach to creating new building blocks.<sup>4,6</sup>

The most challenging derivatives to synthesize among the linear acenes are ones that have their ends but not their edges functionalized. These derivatives are difficult to prepare due to the lack of mild and efficient methods for aromatization and annulation.<sup>8</sup> In contrast, the synthesis of linear pentacycles such as the dihydrodiazapentacenes (**2** and **3**), where nitrogens replaces two of the carbons of pentacene, are efficiently achieved through simple condensation reactions between a 1,2-aromatic diamine and a 1,2-aromatic diol.<sup>1</sup> Particularly attractive are the derivatives in Figure 1c—the 5,14-dihydrodiazapentacenes—

<sup>†</sup> Department of Chemistry, Columbia University.

<sup>‡</sup> DuPont, Central Research and Development.

<sup>§</sup> Current address: School of Engineering, University of Tokyo, 7-3-1 Hongo, Bunkyo-ku, Tokyo 113-8656, Japan.

- (1) (a) Hinsberg, O. *Ann. Chem.* **1901**, 319, 260. (b) Manassen, J.; Khalif, S. *J. Am. Chem. Soc.* **1966**, 88, 1943. (c) Kummer, F.; Zimmermann, H.; *Berichte der Bunsen-Gesellschaft* **1967**, 71(9–10), 1119. (d) Leete, E.; Ekechukwu, O.; Delvigs, P. *J. Org. Chem.* **1966**, 31, 3734.
- (2) Reviews on organic FETs from small molecules: (a) Dimitrakopoulos, C. D.; Malenfant, P. R. L. *Adv. Mater.* **2002**, 14, 99. (b) Katz, H. E.; Bao, Z.; Gilat, S. L. *Acc. Chem. Res.* **2001**, 34, 359. (c) Katz, H. E.; Bao, Z. *J. Phys. Chem. B* **2000**, 104, 671. (d) Horowitz, G. *Adv. Mater.* **1998**, 10, 365. (e) Katz, H. E. *J. Mater. Chem.* **1997**, 7, 369.
- (3) (a) Blanchet, G. B.; Loo, Y.-L.; Rogers, J. A.; Gao, F.; Fincher, C. R. *Appl. Phys. Lett.* **2003**, 82, 463–465. (b) Loo, Y.-L.; Someya, T.; Baldwin, K. W.; Bao, Z.; Ho, P.; Dodabalapur, A.; Katz, H. E.; Roger, J. A. *Proc. Nat. Acad. Sci. (USA)* **2002**, 99, 10 252–10 256. (c) Drury, C. J.; Mutsaers, C. M. J.; Hart, C. M.; Matters, M.; de Leeuw, D. M. *Appl. Phys. Lett.* **1998**, 73, 108–110. (d) Calvert, P. *Chem. Mater.* **2001**, 13, 3299–3305. (e) Voss, D. *Nature* **2000**, 407, 442–444.

- (4) (a) Rogers, J. A.; Bao, Z.; Baldwin, K.; Dodabalapur, A.; Crone, B.; Raju, V. R.; Kuck, V.; Katz, H.; Amundson, K.; Ewing, J.; Drzacic, P. *Proc. Nat. Acad. Sci. (USA)* **2001**, 98, 4835–4840. (b) Roger, J. A.; Bao, Z. *J. Polym. Sci. Pt. A: Polym. Chem.* **2002**, 40, 3327–3334. (c) Huitema, H. E. A.; Gelinck, G. H.; van der Putten, J. B. P. H.; Kuijk, K. E.; Hart, C. M.; Cantatore, E.; Herwig, P. T.; van Breemen, A. J. J. M.; de Leeuw, D. M. *Nature* **2001**, 414, 599.
- (5) Small organic molecules with mobilities approaching amorphous silicon: (a) Lin, Y.-Y.; Gundlach, D. J.; Nelson, S. F.; Jackson, T. N. *IEEE Trans. Elec. Dev.* **1997**, 44, 1325. (b) Li, X. C.; Sirringhaus, H.; Garnier, F.; Holmes, A. B.; Moratti, S. C.; Feeder, N.; Clegg, W.; Teat, S. J.; Friend, R. H. *J. Am. Chem. Soc.* **1998**, 120, 2206–2207. (c) Katz, H. E.; Lovinger, A. J.; Laquindanum, J. G. *Chem. Mater.* **1998**, 10, 457. (d) Laquindanum, J. G.; Katz, H. E.; Lovinger, A. J. *J. Am. Chem. Soc.* **1998**, 120, 664–672. (e) Sirringhaus, H.; Tessler, N.; Friend, R. H. *Science* **1998**, 280, 1741–1744. (f) Katz, H. E.; Lovinger, A. J.; Johnson, J.; Kloc, C.; Siegrist, T.; Li, W.; Lin, Y. Y.; Dodabalapur, A. *Nature* **2000**, 404, 478–481. (g) see ref 2b. (h) see ref 6.
- (6) Meng, H.; Bao, Z.; Lovinger, A. J.; Wang, B.-C.; Mujsce, A. M. *J. Am. Chem. Soc.* **2001**, 123, 9214–9215.
- (7) Matthews, C. C.; Bros, A. B.; Baas, J.; Meetsma, A.; deBoer, J.-L.; Palsera, T. T. M. *Acta Crystallogr.* **2001**, C57, 939–941.

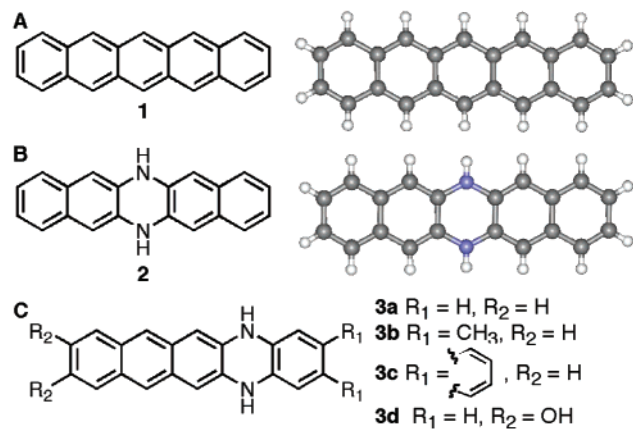
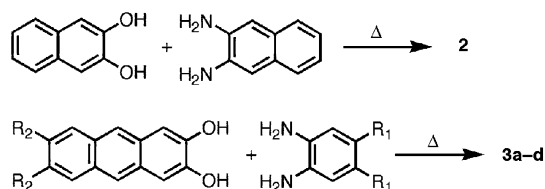


**Figure 1.** (a) Molecular structure and crystal structure of pentacene<sup>7</sup> (**1**); (b) molecular structure and crystal structure of 2, 6,13-dihydrodiazapentacene; and (c) derivatives of 5,14-dihydrodiazapentacene (**3a–d**).

#### Scheme 1



because end-functionalized derivatives are easily generated through the readily available benzene diamines.

#### Results and Discussion

The synthetic scheme that affords the 5,14- and 6,13-dihydrodiazapentacene derivatives is shown in Scheme 1. Full experimental details are available in the Supporting Information, but in general, the products can be crystallized from the reaction mixture. The crystals vary in color for the different derivatives: yellow for **3a** and light green for **2**.

Pentacene is only sparingly soluble in high boiling point aromatic solvents, but **2**, **3a**, and **3d** are soluble in DMF and DMSO at concentrations higher than ca. 1 mg/mL. Moreover, solutions of **2** and **3** that are open to air and light resist oxidation whereas solutions of pentacene are known to degrade in a matter of minutes.<sup>9,17</sup> The origin of the stability of these derivatives has to do with breaking of the conjugation in the pentacene skeleton by interposing the amino functionality. In essence, **2** consists of two naphthalene rings connected by a spacer, and **3** consists of an anthracene ring plus a benzene ring. X-ray diffraction of crystals grown from saturated solutions of **2** in DMF reveals why these derivatives are so soluble. Two molecules of DMF each form a hydrogen bond with the N–H's of **2** as shown in Figure 2a. Interestingly, these three-molecule assemblies further assemble into large nanoscale channels as shown in Figure 2b. From solvents that cannot form hydrogen bonds such as benzophenone, the structure for **2**, changes to a

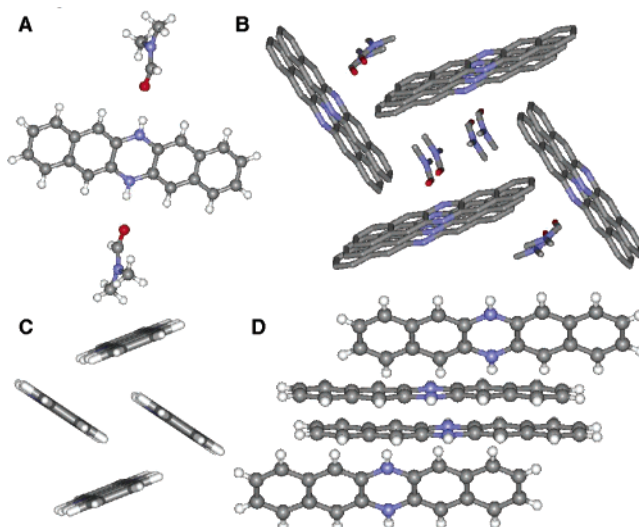


**Figure 2.** (a) Crystal structure of **2** from DMF showing two hydrogen bonds to molecules of solvent; (b) channels through the crystals (hydrogens have been removed to clarify the view); (c) Crystal structure of **2** from hot benzophenone showing a herringbone motif; (d) View of the crystal lattice showing slipping. For the models: gray atoms are carbon, blue atoms are nitrogen, and red atoms are oxygen.

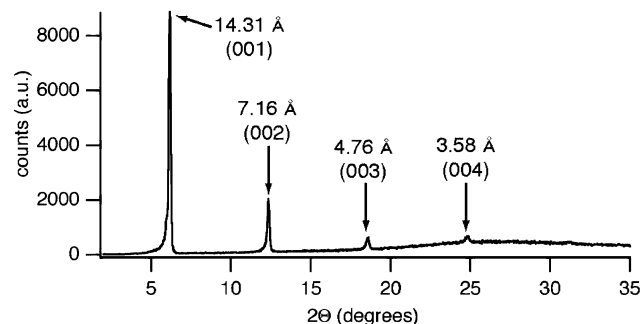


**Figure 3.** X-ray diffraction from a 100 nm film of **3a** on Si/SiO<sub>2</sub>.

herringbone arrangement as shown in Figure 2c. This motif is the characteristic of the packing in pentacene,<sup>7,10</sup> dihydrodiazanthracene,<sup>11</sup> and other electron rich  $\pi$ -systems as predicted by the model of Hunter and Sanders.<sup>12</sup> For **2**, the stacking is slipped relative to pentacene with only four overlapping rings between nearest neighbors in the crystal as shown in Figure 2d. Presumably, this arrangement avoids the energetic penalty of stacking the central dihydropyrazine ring over itself.

Films of these compounds can be grown on oxidized silicon substrates through thermal evaporation in a vacuum. The X-ray diffractograms from films of **2**, **3a**, and **3b** (shown in Figure 3) were similar to each other showing only multiple (00l) reflections. This is also characteristic of films from linear acenes and is attributed to the molecules stacking into layers with the molecule's long axis perpendicular to the surface.<sup>13</sup> The intensity of the X-ray diffraction peaks indicates that the molecules are highly aligned.

(8) Representative syntheses of pentacene and its derivatives: (a) Goodings, E. P.; Mitchard, D. A.; Owen, G. *J. Chem. Soc. Perkin Trans. 1* **1972**, *11*, 1310–1314. (b) Bailey, W. J.; Madoff, M. *J. Am. Chem. Soc.* **1953**, *75*, 5603. (c) Luo, J.; Hart, H. *J. Org. Chem.* **1987**, *52*, 4833–4836. (d) Satchell, M. P.; Stacey, B. E. *J. Chem. Soc.* **1971**, 468. (e) Laquindanum, J. G.; Katz, H. E.; Lovinger, A. J. *J. Am. Chem. Soc.* **1998**, *120*, 664. (f) Anthony, J. E.; Brooks, J. S.; Eaton, D. C.; Parkin, S. R. *J. Am. Chem. Soc.* **2001**, *123*, 9482. (g) Takahashi, T.; Kitamura, M.; Shen, B.; Nakajima, K. *J. Am. Chem. Soc.* **2000**, *122*, 12876–12877. (h) Wartini, A. R.; Staab, H. A.; Neugebauer, F. A. *Eur. J. Org. Chem.* **1998**, *1161*, 1–1170. (9) Yamada, M.; Ikemoto, I.; Kuroda, H. *Bull. Chem. Soc. Jpn.* **1988**, *61*, 1057.

(10) Campbell, R. B.; Robertson, J. M.; Trotter, J. *Acta Crystallogr.* **1961**, *14*, 705–711. (11) Thalladi, V.; Smolka, T.; Gehrke, A.; Boese, R.; Sustmann, R. *New J. Chem.* **2000**, *24*, 143–147. (12) Hunter, C. A.; Sanders, J. K. M. *J. Am. Chem. Soc.* **1990**, *112*, 5525–5534. (13) (a) Gundlach, D. J.; Lin, Y. Y.; Jackson, T. N.; Nelson, S. F.; Schlom, D. G. *IEEE Electron Dev. Lett.* **1997**, *18*, 87–89. (b) Dimitrakopoulos, C. D.; Brown, A. R.; Pomp, A. *J. Appl. Phys.* **1996**, *80*, 2501–2508. (c) Minakata, T.; Imai, H.; Ozaki, M.; Saco, K. *J. Appl. Phys.* **1992**, *72*, 5220–5225.

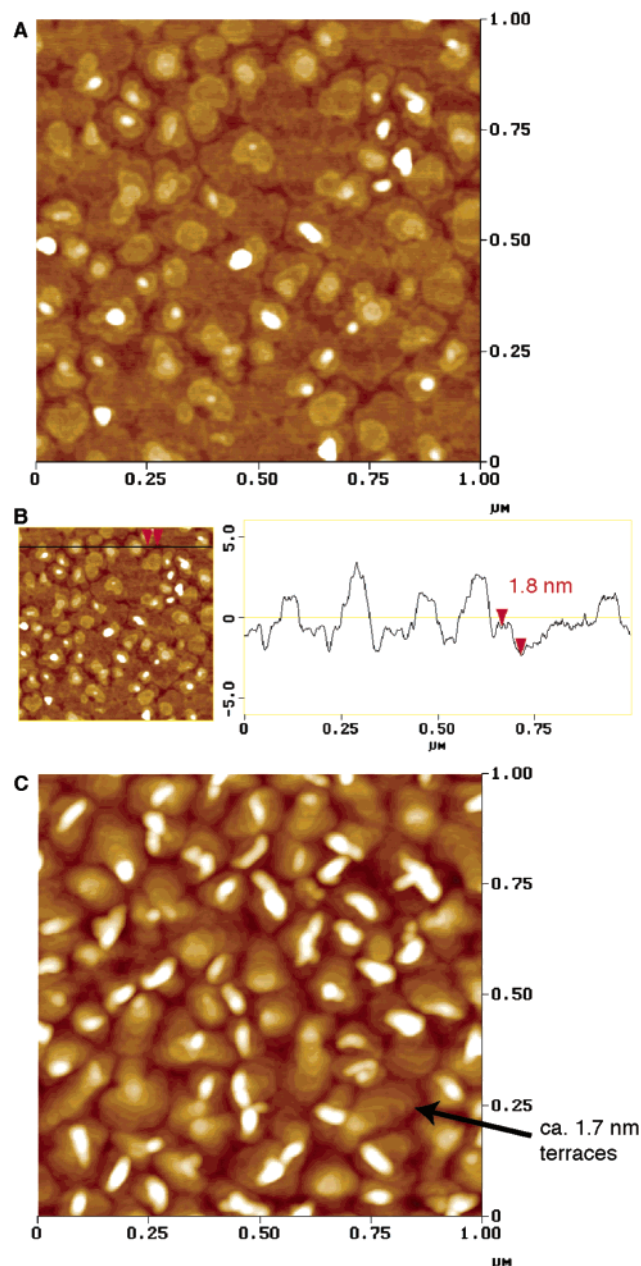


**Figure 4.** (a)  $1 \times 1 \mu\text{m}$  AFM height image of ca. 1.5 nm film of **3a**. (b) Step height in the film in Figure 4a. (c)  $1 \times 1 \mu\text{m}$  AFM height image of ca. 8 nm film of **3a**.

Atomic force microscopy of films of **3a** on Si/SiO<sub>2</sub>, also support this layer-by-layer growth. Shown in Figure 4a is micrograph of a film from a very short deposition time, intended to give a film of approximately one molecular layer in thickness (ca. 1.5 nm). As shown in Figure 4b, each of the steps from the surface in this film are ca. 1.8 nm—roughly the length of the long axis in **3a**. This first layer consists of an intricate set of interconnections that is remarkably different than the dendritic morphology seen in pentacene crystallites.<sup>14</sup> The difference could arise from the dihydrodiazapentacenes having a different balance for its surface diffusion rate and intermolecular attraction. A micrograph of a thicker film (ca. 8 nm) is displayed in Figure 4c. Distinct terraces can be seen in each grain with heights that are consistent with the long axis of the molecule.

(14) Meyer zu Heringdorf, F.-J.; Reuter, M. C.; Tromp, R. M. *Nature* **2001**, *412*, 517–520.

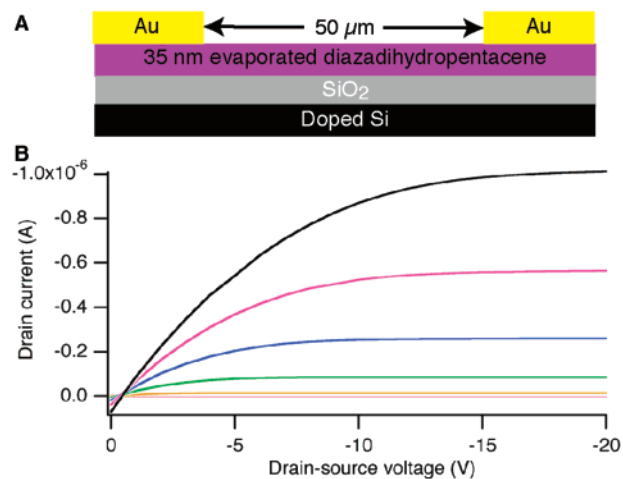


**Figure 5.** (a) Schematic of device configuration for FET's measurements; (b) current/voltage curves for **3a** with varying gate bias (0 to  $-20$  V from red to black in  $-4$  V steps).

The diameter of the grains measured in the AFM micrographs in Figure 4c is ca.  $127 \pm 14$  nm and increases to ca.  $144 \pm 23$  nm for a 35 nm thick film (not shown).

Thermal evaporation of source/drain electrodes onto these polycrystalline films allows field-effect transistor structures to be fabricated with the heavily doped silicon layer functioning as the gate electrode as shown in Figure 5a. The oxide layer was 100 nm thick in these devices and the ratio of the width to the length (W/L) of the channel was 40. Shown in Figure 5b are I–V curves at different gate biases for a ca. 35 nm thick film of **3a**. The film performs as a p-type transistor with a field-effect mobility of  $6 \times 10^{-3} \text{ cm}^2\text{V}^{-1}\text{s}^{-1}$ , which is determined in the saturation regime by using the equation<sup>2</sup>:  $I_{\text{DS}} = (\mu\text{WC}_i/2L)(V_{\text{G}} - V_0)^2$ . On/off ratio of the drain current between 0 and  $-20$  V gate bias was greater than  $10^3$ . With a thicker oxide layer (300 nm) and higher gate voltage ( $-100$  V) the on/off ratio for **3a** could be raised to  $>10^4$ . With the exception of **3d**, which decomposed upon thermal evaporation, all of the other derivatives from Figure 1 behave as organic field effect transistors. Their mobilities and on/off ratios in thermally evaporated films are shown in Table 1. A remarkable feature of devices from **2**, **3a–c** is their atmospheric stability; when they are operated periodically over several days, open to the atmosphere, they show no significant change.<sup>15</sup>

Shown in Figure 6a is a comparison between the UV–vis spectrum of ca. 150 nm films of pentacene and **3a** on quartz substrates. Both materials show sharp band edges suggesting little structural disorder. The longest wavelength transition that is attributed to the band gap is around 670 nm (1.85 eV) for pentacene<sup>16</sup> and around 480 nm (2.58 eV) for **3a**. In pentacene, the transitions at 620 nm (1.98 eV) and 670 nm (1.85 eV) are attributed to Davydov doublet of the 0–0 band and the two other peaks at 540 nm (2.29 eV) and 585 nm (2.13 eV) to the doublet of the 0–1 band.<sup>17</sup> Although the relative intensity of

(15) (a) Hong, X. M.; Katz, H. E.; Lovinger, A. J.; Wang, B.-O.; Raghavachari, K. *Chem. Mater.* **2001**, *13*, 4686–4691. (b) Horowitz, G.; Hajlaoui, R.; Bouchriha, H.; Bourguiga, R.; Hajlaoui, M. *Adv. Mater.* **1998**, *10*, 923. (c) Gundlach, D. J.; Lin, Y.-Y.; Jackson, T. N.; Schlom, D. G. *Appl. Phys. Lett.* **1997**, *71*, 3853–3855.

(16) Kim, K.; Yoon, Y. K.; Mun, M.-O.; Park, S. P.; Kim, S. S.; Im, S.; Kim, J. H. *J. Superconductivity: Incorporating Novel Magnetism* **2002**, *15*, 595–598.

(17) Siebrand, W.; Zgierski, M. Z. *Springer Ser. Solid-State Sci.* **1983**, *49*, 136–44.



**Table 1.** <sup>a</sup> Mobility and On/Off Ratios for **2** and **3a–d** for Transistors Prepared at Different Deposition Temperatures for the Substrate ( $T_s$ )

	$T_s = 17^\circ\text{C}$		$T_s = 60 \pm 3^\circ\text{C}$		$T_s = 90 \pm 1^\circ\text{C}$	
	mobility ( $\text{cm}^2\text{V}^{-1}\text{s}^{-1}$ )	on/off ratio	mobility ( $\text{cm}^2\text{V}^{-1}\text{s}^{-1}$ )	on/off ratio	mobility ( $\text{cm}^2\text{V}^{-1}\text{s}^{-1}$ )	on/off ratio
<b>2</b>	$1 \times 10^{-5}$	200–400	$5 \times 10^{-5}$	$1 \times 10^3$	$2 \times 10^{-6}$	50
<b>3a</b>	$(3\text{--}6) \times 10^{-3}$	$(2\text{--}5) \times 10^3$	$1 \times 10^{-3}$	$2 \times 10^3$	$3 \times 10^{-3}$	$2 \times 10^3$
<b>3b</b>	$(3\text{--}4) \times 10^{-4}$	100	$1 \times 10^{-3}$	500–700	$(6\text{--}8) \times 10^{-4}$	100–500
<b>3c</b>	no field effect	$2 \times 10^{-4}$	$3 \times 10^3$	$5 \times 10^{-4}$	$4 \times 10^3$	

<sup>a</sup> The thickness of the gate dielectric layer ( $\text{SiO}_2$ ) was 100 nm and the on/off ratios were measured between gate biases of 0 and  $-20$  V.

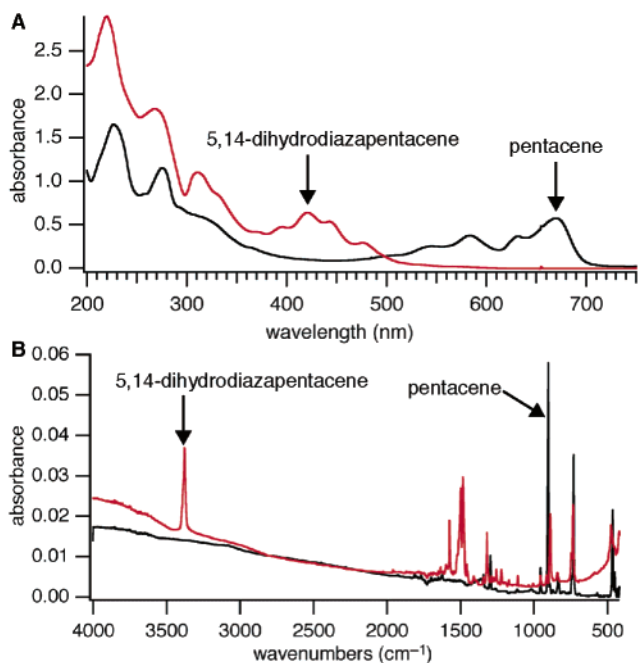


**Figure 6.** (a) UV-vis spectrum of **3a** (red trace) compared to pentacene (black trace). (b) Infrared spectrum of **3a** (red trace) compared to pentacene (black trace).

the peaks is different, **3a** also has four long wavelength transitions that could be assigned as the two sets of Davydov doublets: the 0–0 band at 445 nm (2.78 eV) and 480 nm (2.58 eV); the 0–1 band at 395 nm (3.14 eV) and 420 nm (2.95 eV). The Davydov components are polarized in the plane that is defined by the two short axes of the molecule (the a,b-plane), indicating that this plane is parallel to the substrate—the molecule's long axis is upright from the surface. This conclusion is in agreement with the X-ray diffraction and AFM results in Figures 4 and 5.

The longest wavelength absorption for pentacene is red-shifted by ca. 80 nm on going from solution<sup>18</sup> or the gas phase<sup>19</sup> to thin film due to the association between the molecules in the solid state.<sup>16,17</sup> By contrast, the red shift for **3a** is only around 10 nm going from a THF solution to a film. This low amount of shifting for **3a** upon film formation coupled with these films intense fluorescence makes them viable candidates for LED

(18) In solution: *UV Atlas of Organic Compounds*; Plenum Press: New York, 1966, Vol. 3.

(19) In an argon matrix: (a) Szczepanski, J.; Wehlburg, C.; Vala, M. *Chem. Phys. Lett.* **1995**, *232*, 221. (b) Halasinski, T. M.; Hudgins, D. M.; Salama, F.; Allamandola, L. J.; Bally, T. *J. Phys. Chem. A* **2000**, *104*, 7484.

applications. Moreover, these films do not show any evidence for photooxidation that occurs readily in films of pentacene.<sup>20</sup> A comparison of the infrared spectra from **3a** and pentacene on KBr substrates is displayed in Figure 6b. The intense IR bands at 730 and 908  $\text{cm}^{-1}$  in films of pentacene that correspond to out of plane H-movement shift only slightly to 736 and 889  $\text{cm}^{-1}$  for **3a**. The additional strong bands at 3378 and 1500  $\text{cm}^{-1}$  for **3a** correspond to N–H stretching and bending, respectively.

## Conclusion

In summary, these studies demonstrate that dihydrodiazopentacenes self-assemble into polycrystalline films that can form the active layer in a FET device. The on/off ratios are sufficiently large that some of the derivatives synthesized here could find utility as drivers for organic displays. These materials have several other advantages relative to pentacene: they are easily derivatized, environmentally stable, and also somewhat soluble. One very promising application of small molecule organic FETs is in chemical and vapor sensing applications.<sup>21</sup> The amine functionality of the dihydrodiazopentacenes films could serve both as a hydrogen bond donor and a site for derivatization providing analyte specificity in these sensors.

**Acknowledgment.** This work is supported primarily by the Nanoscale Science and Engineering Initiative of the National Science Foundation under NSF Award Number CHE-0117752. We also acknowledge financial support from the Chemical Sciences, Geosciences and Biosciences Division, Office of Basic Energy Sciences, US D.O.E. (No. DE-FG02-01ER15264). C.N. thanks the Beckman Young Investigator Program (2002) and the Dupont Young Investigator Program (2002) for financial support. We thank Prof. Parkin (Columbia) and Dr. Kevin Janak (Columbia) for solving the X-ray structures in Figure 2.

**Supporting Information Available:** Details for the synthesis of **2** and **3**, the device preparation, the electrical measurements, and the crystal structure data. This material is available free of charge via the Internet at <http://pubs.acs.org>.

JA036466+

(20) Kamura, Y.; Shirotani, I.; Inokuchi, H.; Maruyama, Y. *Chem. Lett.* **1974**, *6*, 627–30.

(21) (a) Crone, B. K.; Dodabalapur, A.; Sarpeshkar, R.; Gelperin, A.; Katz, H. E.; Bao, Z. *J. Appl. Phys.* **2002**, *91*, 10 140–10 146. (b) A. Assadi, A.; Gustafsson, G.; Willander, M.; Svensson, C.; Inganäs, O. *Synth. Met.* **1990**, *37*, 123. (c) Guillaud, G.; Simon, J.; Germain, J. P. *Coord. Chem. Rev.* **1998**, *178*, 1433. (d) Torsi, L.; Dodabalapur, A.; Sabbatini, L.; Zambonin, P. G. *Sens. Actuators B* **2000**, *67*, 312. (e) Crone, B.; Dodabalapur, A.; Gelperin, A.; Torsi, L.; Katz, H. E.; Lovinger, A.; Bao, Z. *Appl. Phys. Lett.* **2001**, *78*, 2229.